The valveless diffuser pump – a numerical design study using MATLAB

Anders Olsson*, Göran Stemme and Erik Stemme

Department of Signals, Sensors and Systems, Royal Institute of Technology, SE-100 44 Stockholm, Sweden
* Present address: IMC - Industrial Microelectronics Center, Electrum 233, SE-164 40 Kista, Sweden
Phone: +46 8 752 1000, Fax: +46 8 750 5430, E-mail: anders.olsson@imc.kth.se

ABSTRACT

A lumped-mass model is used to improve the design of the valveless diffuser pump. The model is implemented using MATLAB and tested for different previously reported pumps. The flow-pressure characteristics are predicted for different excitation levels. It is seen that low chamber pressure limits the possible excitation level. A pump with two serially connected pump chambers working in anti-phase is found advantageous compared with a single chamber pump. Indication is found that down scaling of the diffuser elements from 80×80 µm throat cross-sectional area to 40×40 µm throat cross-sectional area increase the attainable pressure head. The possibility to use deposited PZT instead of discs fixed with adhesive is shown promising.

INTRODUCTION

The valveless diffuser pump is based on the diffuser element's direction dependent flow resistance [1-4]. The basic unit of the pump is shown in Figure 1. It consists of two diffuser elements connected to a pump chamber with an oscillating diaphragm. In the figure, the diffuser elements are connected in series with flow channels. During the supply mode, more fluid flows through the inlet element than through the outlet element and during the pump mode more fluid flows through the outlet element than through the inlet element. The result is a net flow from the inlet side to the outlet side.

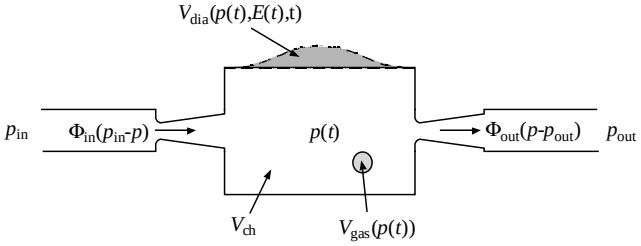

Figure 1. The basic unit of a diffuser pump.

A simple analytic model has been developed [2] that estimates the resonance frequency of the pump where the diaphragm is the spring and the mass is fluid in the diffuser elements. The continuity equation was used to formulate an approximate expression for the volume flow. The latter was recently further extended to include the pressure behavior [5], but without including inertial effects and consequently the relation between the geometry and the resonance frequency was not considered.

To further optimize the valveless diffuser pump a better model is necessary. The common way to model micropumps is to use lumped-mass models, i.e., the structure is divided into lumped mass elements. These elements can be described individually by simple analytic models and simple relations can be formulated between the individually elements [6]. This approach has been used in, e.g., [7-10]. During this work a lumped-mass model is developed especially for the valve-less diffuser pump. The model is verified using experimental results for different pumps [1, 2, 4] and new designs are suggested.

THE LUMPED MASS MODEL

The model is formulated based on the unit shown in Figure 1. The inlet and outlet pressures are assumed constant. The model includes stiffness, masses and viscous losses and is able to handle nonlinearities. The following description is a summary of what is extensively described in [11, 12].

An equation for the diaphragm is formulated using Newton's second law. For the previously tested liquid pumps [1-4] the mass of the diaphragm is negligible compared with the other masses in the system. The equation for the diaphragm can then be written as

$$\dot{V}_{dia} = \partial V_{dia} / \partial E \cdot \dot{E} + \partial V_{dia} / \partial p \cdot \dot{p} \qquad (1)$$

where V_{dia} is the volume change due to deflection of the diaphragm, $\dot{V}_{dia}$ is dV_{dia}/dt, t is the time, p is the chamber pressure and E is the electric field strength across the piezoelectric disc used for the actuation.

The conservation of mass law [13] is used on the chamber volume. Assuming a stiff chamber and that the chamber volume, V_{ch}, is much larger than V, the equation can be expressed as

$$\frac{dp}{dt} = \frac{\Phi_{in}(p_{in}-p) - \Phi_{out}(p-p_{out}) - \partial V_{dia}/\partial E \cdot \dot{E}}{\frac{\partial V_{dia}}{\partial p} + \kappa_{liquid} V_{ch} + \left(\frac{1}{p+p_0} - \kappa_{liquid}\right) \cdot \frac{x \cdot V_{ch} \cdot p_0}{p+p_0}} \qquad (2)$$

where Φ_{in} and Φ_{out} are the flows through inlet and outlet, p_{in} and p_{out} is the pressure at inlet and outlet, κ_{liquid} is the compressibility of the liquid which is assumed constant, p_0 is the pressure outside the chamber and x is the relative gas content (V_{gas}/V_{ch}) in the chamber at the pressure p_0. The gas is assumed ideal.

A flow channel of arbitrary shape can be analyzed using the energy equation for a fixed control volume. For a channel, where the flow, Φ, can be assumed one-

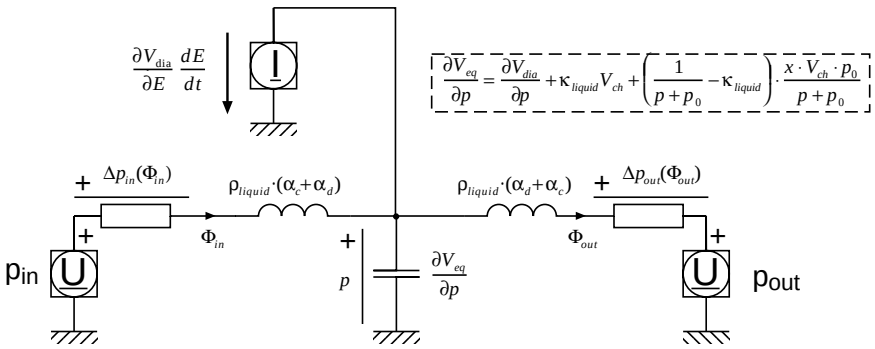

Figure 2. An electric circuit illustrating the simplest form of the valve-less diffuser pump.

dimensional and for which the cross-sectional areas and velocity profiles at inlet and outlet are the same, the equation can be written

$$p_{in} = p_{out} + \rho\alpha \cdot \dot{\Phi} + \Delta p_{loss} \tag{3}$$

there α depends on the velocity profile and Δp_{loss} is the pressure drop due to viscous losses. For a channel with the constant cross-sectional area, *A*, and the length *L,* a flat flow profile gives $\alpha = L/A$. This differs from that for a turbulent flow profile with only 2 percent.

The diaphragm mass is negligible compared to the mass in the diffuser elements and the mass inside the chamber are also neglected. The resulting equation system is illustrated as an electric circuit in Figure 2. It was solved using MATLAB®. The model can easily be extended for other configurations including more chambers, buffer elements and flow channels.

The flow losses in the diffuser elements are based on results from steady flow measurements fitted to polynomial using a least square fit of coefficients k_1, k_2, k_3 and k_4 in the expression for the pressure drop Δp_{model}

$$\Delta p_{\text{model}} = \begin{cases} C_1 \cdot \left(k_1 \cdot \Phi + k_2 \cdot \Phi^{7/4}\right), & \Phi \geq 0 \\ C_2 \cdot \left(k_3 \cdot \Phi + k_4 \cdot \Phi^{7/4}\right), & \Phi < 0 \end{cases} \tag{4}$$

where Φ is the flow. The losses for dynamic flow can be expected to be different from steady flow [14]. To account for this and other non-included effects two more coefficients, C_1 and C_2, were added.

For other parts the flow losses, Δp , are calculated using the law of friction for laminar flow [14]

$$\Delta p = 0.5 \cdot c \cdot L \cdot \eta \cdot \bar{u} / D_h^2 \tag{5}$$

where c is a parameter depending on the geometric shape, L is the channel length, η is the viscosity, $\bar{u}$ is the mean velocity and the hydraulic diameter, D_h, is calculated as $D_h = 4 \cdot \text{Area}/\text{wetted peimeter}$. For flow through a circular cross-section, *c* can be determined analytically to be 64. For rectangular cross-sections data are found in, e.g., [13].

SIMULATIONS

The model was implemented in MATLAB and tested for several previously experimentally evaluated pumps [1, 2, 4]. Their dimensions are given in Table 1. All the pumps have been tested using water as liquid. For all pumps the

Table 1. Data for the investigated valve-less diffuser pumps.

	The conical brass pump (A) [1]	The conical brass pump (B) [1]	The flat-walled Brass pump [2]	The flat-walled silicon pump		
				Diffuser width		
				80 µm [4]	40 µm (not tested)	20 µm(not tested)
Chamber radius [mm]	9.5	9.5	6.5	3.0	3.0	3.0
Diaphragm thickness [mm]	0.2	0.2	0.35	0.42	0.42	0.42
PZT disc radius/thickness [mm]	8.0/0.2	8.0/0.2	5.0/0.2	1.9/0.2	1.9/0.2	1.9/0.2
Depth [µm]	≈ 500	≈ 500	300	80	40	20
Diffuser element throat diameter/width [µm]	230	530	300	80	40	20
Diffuser element outlet diameter/width [mm]	0.60	1.10	1.00	0.267	0.133	0.067
Length diffuser [mm]	4.0	3.0	4.1	1.093	0.547	0.273
Channel diameter/width[mm]	2.80	2.80	3.0	2.0	2.0	2.0
Channel length [mm]	2.0	2.0	10	3.6	3.6	3.6
$\partial V/\partial p$ / 10^{-17}	4910	4910	390	3.12	3.12	3.12
$\partial V/\partial E$ / 10^{-18}	1110	1110	290	2.22	2.22	2.22
Measured frequency [Hz]	110	310	540	3350	-	-
Calculated frequency [Hz] [2]	165	392	734	4238	2997	2119
Simulated frequency [Hz]	160	350	600	3500	2650	1619
$C_{diffuser} = C_1$; $C_{nozzle} = C_2$	1; 1	0.6; 1	0.8; 1.2	0.5; 1.6	0.5; 1.6	0.5; 1.6

diaphragm properties were calculated using a finite element program (ANSYS). The values used for the simulations are given in Table 1. All experiments were done using a square wave voltage for excitation. For the numerical simulations, this will cause difficulties with dE/dt and instead a sinusoidal signal was assumed. This should not significantly affect the results since the pumps are operated at their resonance frequencies.

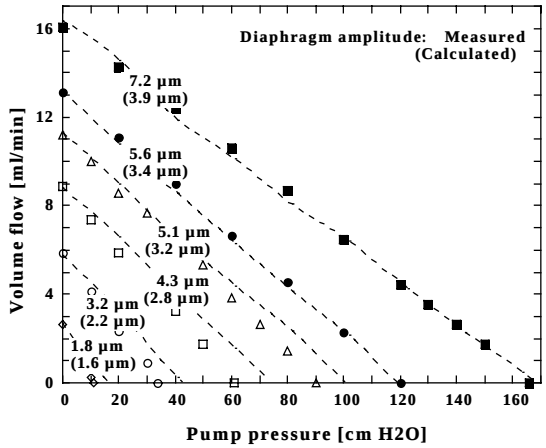

Figure 3. Measured (symbols) [2] and calculated (dashed lines) flow-pressure characteristics for the Flat-walled Brass Pump.

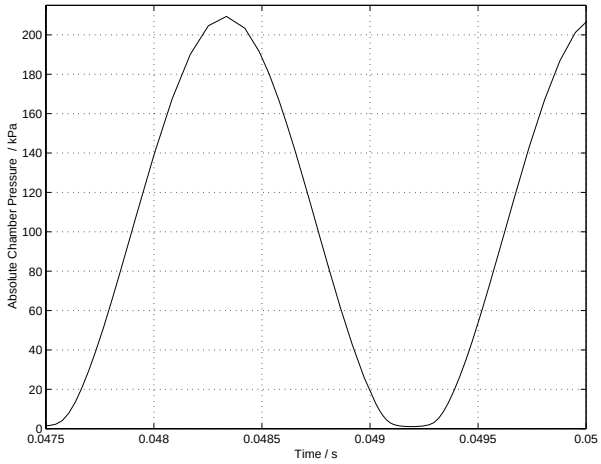

Figure 4. The calculated chamber pressure inside the Flat-walled Brass Pump at the highest excitation level and zero pressure head.

The simulations were done in the order that first the frequency for maximum volume flow was determined. Then the excitation level and the coefficients C_1 and C_2 were adjusted to fit the measured volume flow and pressure head. The procedure was repeated until the result was satisfying. The differences between the simulated and measured resonance frequencies can be explained by the differences in the real velocity profile compared with the flat profile used in simulations. All simulations were done assuming an air content of 10 ppm in the chamber liquid [15].

The flow-pressure characteristics for the conical brass pump and the flat-walled brass pump show similar behavior. For the latter, it is shown in Figure 3. The simulations were done using the simple model and the simulated flow was doubled to correspond to a double chamber pump. The excitation levels were chosen to correspond to the measured volume flow and then the lines were calculated for a number of points. The simulations show that there is a difference between the calculated and measured diaphragm amplitudes. Tests showed that this probably mainly was dependent on problems with the measurement equipment.

The simulated absolute pump chamber pressure is shown in Figure 4 for the flat-walled brass pump. The chamber pressure goes towards zero at the maximum excitation level. The calculated minimum chamber pressure is about 0.6 kPa. Compared with the vapor pressure for water of approximate 2.3 kPa at 20ºC this indicates that low chamber pressure limits the pump performance [16].

Figure 5 shows plots of the volume flow and pressure head versus the frequency for the same excitation level (80 V p-p for the measurements). The simulated frequency behavior is very similar to the measured. Simulation of the volume flow and pressure head versus the diaphragm amplitude also showed behavior very similar to the measurements. For the flow the relation is linear and for the pressure it is a second degree polynomial.

The flat-walled silicon pump presented in [4] is simulated using a single chamber model. The result is shown in Figure 6 together with measured values. The figure also shows simulations for several other configurations: a serial pump operated in in-phase and anti-phase mode and pumps with the diffuser element dimensions scaled down to 40×40 µm^2 and 20×20 µm^2 throat cross-section. The chamber depth is equal to the diffuser depth. The stationary flow-pressure characteristics were assumed to scale as between the flat-walled brass pump and the flat-walled silicon pump.

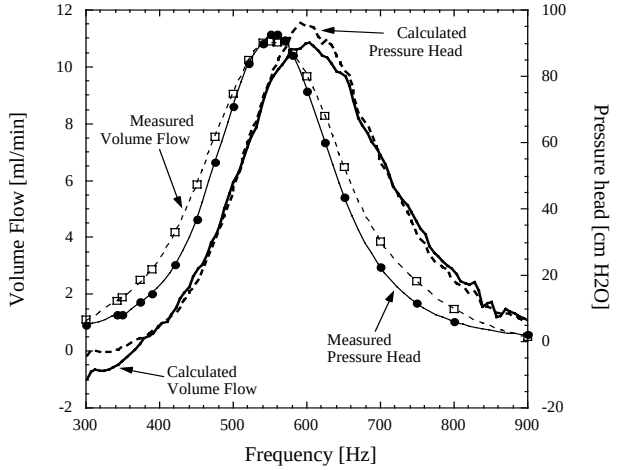

Figure 5. Maximum volume flow and pressure head vs. the frequency for the Planar Pump. The excitation level for the measurements was 80 V p-p.

The calculations for a pump using deposited PZT was based on the design of the pump with 40×40 µm cross-section described above. The diaphragm properties were

calculated using approximate analytic formulas for the deflection of a plate under thermal load [17] with the thermal expansion coefficient, γ, replaced with the piezoelectric charge constant, d_{31}. The PZT was assumed to have a Young's modules of 60 MPa, Poisons ratio of 0.3 and d_{31}=-70pm/V. For silicon 150 MPa was used for Young's modules and 0.17 for Poisons ratio. The simulated pump performances are shown in Figure 7 with the chamber radius equal to the diaphragm radius. An electric field strength of 500 V/mm was used. The simulations indicate that such pumps should work. It is probably possible to fabricate a working pump using a PZT thickness of only 10 µm. The excitation level is limited of the allowed electric field strength. The piezoelectric charge constant, d_{31}, should be as high as possible. The assumed -70 pm/V is significantly lower than -200 pm/V for the piezoelectric ceramic PXE5 from Philips Components. The simulations in Figure 7 shows the best performance for the pump with a 100 µm thick silicon diaphragm almost completely covered by deposited PZT.

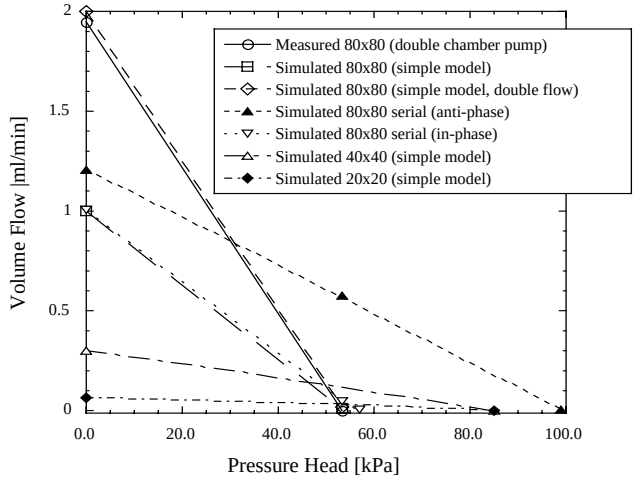

Figure 6. Measured and calculated flow-pressure characteristics for the Flat-walled Silicon Pump.

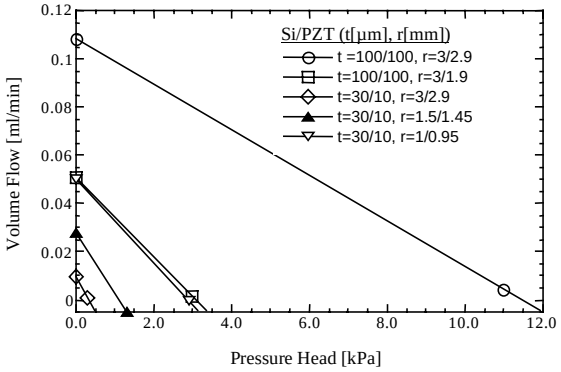

Figure 7. Simulated pump performance for pumps with deposited PZT.

CONCLUSION

The presented lumped-mass model describes the valve-less diffuser pump satisfactory and is useful improve the design. The results indicate that low chamber pressure limits the maximum excitation level. The pressure head can be increased by using a pump with two serial connected chambers operated in anti-phase. The pressure head can probably be further increased by scaling down the diffuser elements dimensions. The performance is highly dependent on flow-pressure characteristics of the diffuser elements and they need to be optimized to optimize the pump.

The study indicates that deposited PZT probably can be used for actuation of the pump. A working pump can be achieved for a 10 µm thick PZT layer. The geometry for the diaphragm and the PZT is important. This is seen in Figure 7 where a 30 µm thick diaphragm almost completely covered with 10 µm thick PZT gives the same pump performance as a 100 µm thick diaphragm partly covered with 100 µm thick PZT. Further, the piezoelectric charge constant, d_{31}, should be as high as possible. The excitation level is limited of the allowed electric field strength.

ACKNOWLEDGMENT

This work was partly founded by Swedish National Board for Industrial and Technical Development (NUTEK) and partly by the European Community under the Industrial and Materials Technologies Programme (Brite - Euram III).

REFERENCES

[1] Stemme *et al*, Sensors and Actuators A39 (1993) 159-67.
[2] Olsson *et al*, Sensors and Actuators A46-7 (1995) 549-56.
[3] Olsson *et al*, J. Micromech. Microeng., 6 (1996) 87-91.
[4] Olsson *et al*, J. Microelectromech Syst., 6 (1997) 161-6.
[5] Ullman, Sensors and Actuators, vol. A69 (1998) 97-105.
[6] Gravesen *et al*, J. Micromech. Microeng., 3 (1993) 168-82.
[7] Voigt *et al*, Sensors and Actuators A, 66 (1998) 9-14.
[8] F. C. M. van de Pol, Thesis: A pump based on micro-engineering techniques, University of Twente, Enschede, the Netherlands, 1989
[9] Zengerle *et al*, J. Micromech. Microeng., 4 (1994) 192-204.
[10] Bardell *et al*, "Designing High-performance Micro-pumps Based on No-moving-parts Valves," Microelectromechanical Systems (MEMS) ASME 1997, DSC-Vol. 62/HTD-Vol. 354, 1997, pp. 47-53.
[11] Olsson *et al*, J. Micromech. Microeng., 9 (1999) 34-44
[12] A. Olsson, Ph.D. Thesis: Valve-less Diffuser Micropumps, Royal Institute of Technology, Stockholm, Sweden, 1998
[13] F. M. White, Fluid Mechanics. New-York: McGraw-Hill, Inc., 1986.
[14] H. Schlichting, Boundary-layer theory, 7th ed. New-York: McGraw-Hill, Inc., 1979.
[15] D. S. Miller, Internal flow systems, 2 ed. Houston, Texas: Gulf Publishing Company, 1990.
[16] R. C. Weast, Handbook of Chemistry and Physics, 53rd ed. Cleveland, Ohio: CRC Press, 1972.
[17] W. C. Young, Roark's Formulas for Stress & Strain, 6 ed. New York: McGraw-Hill, Inc., 1989.